

APPLYING NEATM TO LUNAR SUBSOLAR SPECTRA IN SEARCH OF HYDRATION FEATURES

A. Waiters¹, H. Kaluna¹, D. Takir², P. Smith¹, P. Lucey³, C. Honnibal³, C. Ferrari Wong³, A. Flom³, ¹Physics and Astronomy, University of Hawaii at Hilo, HI, ²JETS/ARES, NASA JSC, Houston, TX, ³Institute of Geophysics and Planetology, University of Hawaii, at Manoa, Manoa, HI

Introduction: A variety of space-based and ground-based observations indicate the presence of OH/H₂O on the surface of the Moon [e.g. 1-6]. Nonetheless, the origin of this surface water and the nature of its distribution and transport are still poorly understood. In addition to differences observed between Lunar Prospector hydrogen maps and M³ data [1], variations in 3- μ m spectral data and thermal models have also resulted in conflicting trends in the distribution of surficial OH/H₂O [7,8]. The latter is in part due to the sensitivity of 3- μ m absorption features to derived surface temperatures and thermal emission corrections. The lack of correlation between derived temperatures and thermal models is greatest near regions of low solar incidence angles, and the 3- μ m feature has been suggested to persist even at the warmest temperatures [7]. Thus, the characterization of the 3- μ m absorption feature near the subsolar region is of particular interest.

This study uses data from a ground-based observing campaign along with the Near-Earth Asteroid Thermal Model (NEATM) [9] to employ an alternative thermal modeling approach in characterizing the presence of OH/H₂O at the subsolar point.



Figure 1: Locations corresponding to subsolar point observations where groundbased spectra were taken using the NASA IRTF. Dates and observing geometry for these points and observations are given in Table 1.

Methods and Results: Ground-based data of the Moon were collected using the NASA Infrared Telescope Facility (IRTF) and the near-IR spectrograph

Obs. Point	Date	Latitude, Longitude	α (°)	r (AU)	Δ (AU)
1	190326	-1.489°, 294.60°	72.32°	0.9983	0.0026
2	180627	-0.827°, 12.95°	9.84°	1.0192	0.0027
2	180627	-0.826°, 12.26°	9.46°	1.0190	0.0027
3	180626	-0.848°, 24.80°	20.75°	1.0190	0.0026
3	180626	-0.848°, 24.79°	20.71°	1.0190	0.0026
4	190714	0.139°, 34.88°	29.34°	1.0188	0.0026
5	190515	-1.270°, 48.93°	46.98°	1.0124	0.0024

Table 1: Dates and observing geometries (α - phase angle, r - heliocentric distance, Δ - geocentric distance) for subsolar observations.

SpeX. The LXD_short mode was used to achieve a spectral coverage of 1.67 - 4.2 μ m and a 1 - 2 km spatial resolution. Spectra of the subsolar point were collected on five different nights (Figure 1 and Table 1) and to avoid saturation, the narrowest slit (0.3" x 15") and the shortest exposures (~0.5 seconds) were used. For each observation, a solar-like standard star was observed at similar airmasses immediately after or prior to observations of the Moon.

Data reduction and calibrations were performed using the IDL-based Spextool (v4.0) program [10,11]. Flat-field correction and wavelength calibration were performed, and an extraction aperture of 1" was used for both the standard star and lunar data. For each observation, at least 10-20 spectra were obtained of the

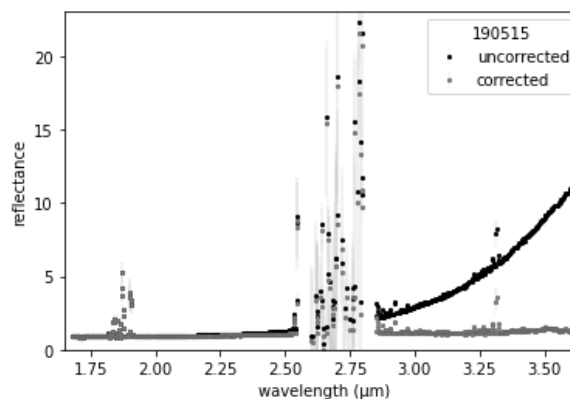


Figure 2: The reflectance spectra of the subsolar point (uncorrected) and the thermally corrected spectrum for data collected on June 15, 2019.

standard star and the subsolar point. The final reflectance spectrum was produced using the average lunar and standard star spectra (see Figure 2).

Near Earth Asteroid Thermal Model: To provide an alternative test of the 3- μm feature's behavior at the subsolar point, we employ NEATM to model the thermal excess of the lunar data. The model is a variation of the Standard Thermal Model (STM) [12], which assumes no thermal emission arises on the night side of the object. The object is also assumed to be an idealized non-rotating sphere, where at 0° phase angle the temperature distribution decrease from the maximum at the subsolar point to zero at the terminator. The STM allows us to find the observed Temperature (T):

$$T(\omega) = T_{Max} \cos^{1/4}(\omega)$$

for $0 \leq \omega \leq \frac{\pi}{2} \leq$ where ω is the subsolar-Earth angle, and the subsolar temperature T_{Max} is given by:

$$T_{Max} = [S(1 - A)/\eta\epsilon\sigma]^{1/4}$$

Where A is the bolometric bond albedo, S is the incident Solar Flux, ϵ is the emissivity, η is the beaming parameter, and σ is the Stefan-Boltzmann constant. Being an extension of the STM, the NEATM uses the beaming parameter as a calibration parameter, in which it is varied until the best fit to the thermal excess is found. The solar phase angle is also considered by calculating the thermal flux an observer would detect from the illuminated portion of a smooth sphere visible at a given solar phase angle, instead of using a fixed phase coefficient as done in the standard model.

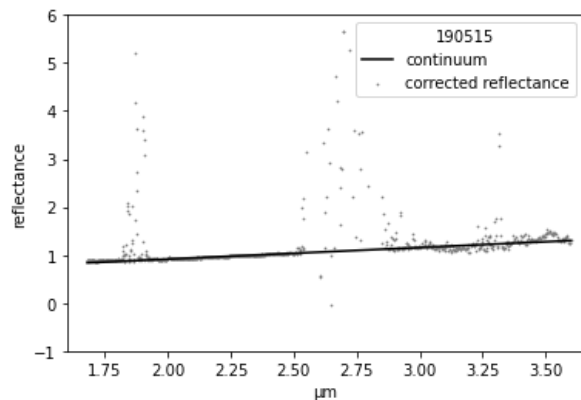


Figure 3: The continuum line (solid) is shown along with the thermally corrected reflectance spectrum. No significant band depth was measured. Data are from June 15, 2019.

Band Depth Analysis: We calculate 3- μm band depths, D , using the following equation:

$$D = \frac{R_c - R_\lambda}{R_c}$$

where R_c is the reflectance at wavelength λ , and R_λ is the reflectance of the continuum at the same wavelength. The continuum is determined by using a linear fit between 2.0 and 2.5 μm and extrapolated across the full spectral range of the data (see Figure 3). We determine the band depth as the average of 5 points centered around 3- μm , and measure uncertainty using the standard deviation of the 5 reflectance values. The preliminary band depth values reported in Table 2 shows no evidence of a 3- μm OH/H₂O absorption band present in our subsolar data.

Obs. Point	Date	Band Depth (D)
1	190326	-0.062 ± 0.085
2	180627	0.016 ± 0.012
2	180627	-0.13 ± 0.039
3	180626	-0.051 ± 0.075
3	180626	-0.045 ± 0.081
4	190714	-0.024 ± 0.044
5	190515	-0.007 ± 0.021

Table 2: 3- μm band depth measurements for the lunar subsolar points observed with NASA IRTF. Negative values indicate excesses above the continuum.

Conclusions: To further explore the presence of water and its temporal variations at the subsolar point, ground-based near-IR spectra were taken of the subsolar point at 5 distinct locations on the Moon. Additionally, an approach often used in characterizing hydration features on asteroids [11] was used as an alternative method for modeling thermal excesses in the lunar data. Regardless of the location on the lunar surface, we find that the 3- μm OH/H₂O absorption band is not evident at any of the subsolar points.

References:

- [1] Pieters C.M. et al. (2009) *Science* 326, 568. [2] Sunshine J.M. et al. (2009) *Science* 326, 565. [3] Clark R.N. (2009) *Science* 326, 562. [4] Feldman, W. C. et al. (1998). *Science*, 281,1496-1500. [5] Honniball, C. I., et al. (2020). *JGR: Planets*, 125(9). [6] Honniball, C. I., et al. (2021). *Nature Astronomy*, 5(2), 121-127. [7] Bandfield, J. L., et al. (2018). *Nature geoscience*, 11(3), 173-177. [8] Li, S., & Milliken, R. E. (2017). *Science advances*, 3(9) [9] Harris, A. W. (1998). *Icarus*, 131(2), 291-301. [10] Cushing C. C. et al. (2004) *PASP* 116, 362 [11] Vacca W. D. et al. (2003) *PASP* 115, 389. [12] Lebofsky, L. A., et al. (1986) *Icarus* 68, 239-2.